Simulation of footings under inclined loads using different constitutive models

J. Hintner, P.A. Vermeer
Institute of Geotechnical Engineering, University of Stuttgart, Germany

P.-A. von Wolffersdorff
Baugrund Dresden Consulting Engineers, Dresden, Germany

ABSTRACT: Two different constitutive models are used for the numerical simulation of footings, namely an elastoplastic model as developed at the University of Stuttgart and a hypoplastic model as developed at the University of Karlsruhe. Both models have been extended to include high soil stiffnesses at very low strain levels and it will be shown that this significantly improves the quality of FE predictions of footings under load. Without such an extension both models tend to overestimate settlements; in particular for plane strain strip footings. In classical settlement analyses the small-strain stiffness is not used and they thus tend to overestimate settlements. This effect is reduced by the introduction of a so-called "limit depth". The classical "limit depth" criterion will be discussed and compared to data from FE-analyses.

In the second part of this paper attention is focused on inclined loads. Computational results are also discussed for inclined failure loads, but the emphasis is on (horizontal) displacements under working loads. In analogy to the simple elasticity method as often used for practical settlement analyses, we consider such a formula for the horizontal displacement. No doubt, the difficulty is to assess an appropriate Young`s Modulus for use in such a formula, as also discussed in this paper.

1 INTRODUCTION

Numerical calculations have been carried out with the elastoplastic Hardening-Soil model developed at the University of Stuttgart and the hypoplastic model developed at the University of Karlsruhe. Both models are nowadays extended to include small-strain stiffness effects. Both models have been calibrated by Hintner et al (2006) on the basis of high quality experimental data from oedometer and triaxial tests.

It was already shown by Hintner et al. (2006) that the comparison between two completely different constitutive numerical models gave a good agreement on the load-settlement curves for a strip footing as well as circular footing. In section 4 the importance of considering the effects of the high stiffnesses at very low strain levels in numerical analysis will be highlighted.

In section 5 the ultimate load envelope for inclined loads using the above-mentioned soil models will be presented. The computed ultimate loads also will be compared to conventional geotechnical design for the bearing capacity problem such the German code of practice.

In section 6 the horizontal displacement under inclined loads will be discussed. The horizontal load-horizontal displacement curves are then compared to the results of an analytical method able to predict horizontal displacements due to horizontal loads. This method was described by Giroud (1969) for an elastic halfspace. We extended it to cover finite layers.

2 CONSTITUTIVE SOIL MODELS

The elastoplastic Hardening-Soil model goes back to the double hardening model as published by Vermeer (1978). Schanz (1998) created a similar model by using a Mohr-Coulomb type yield surface instead of a Matsuoka & Nakai type one and by introducing user-friendly input parameters. Most recently this model was extended by Benz (2006) to account for small-strain soil behaviour. Both the HS model and the HS-small model, i.e. the newest extension by Benz have been implemented in the Plaxis finite element code.

The hypoplastic model as also used in this study goes back to the original work of Kolymbas (1991). In 1996 a hypoplastic model with a predefined limit state surface taking Matsuoka & Nakai criterion was published by von Wolffersdorff. Later this constitutive model was extended by Niemunis & Herle (1997) to include the so-called small-strain stiffness.

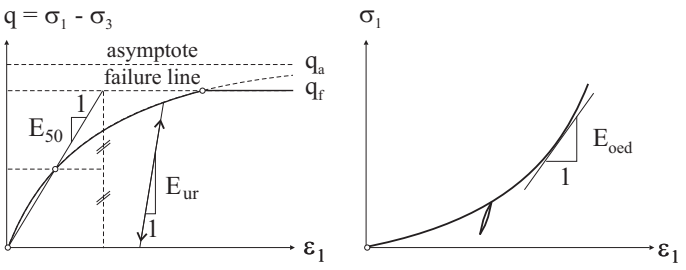

Figure 1. Characteristic curve of a drained triaxial test (left) and an oedometer test (right).

3 INPUT DATA FOR THE SOIL

Calculations of a strip footing have been performed for loose and dense Hostun sand. The soil parameters were obtained by calibrating them on the basis of oedometer and triaxial tests. Good fitting between experimental data and numerical simulations was shown by Hintner et al. (2006) both for triaxial and oedometer test data. The parameters for the HS-small model and the hypoplastic model are given in Tables 1 and 2 respectively. The stiffnesses for the HS-(small) model are given at a reference pressure of p_{ref} = 100 kN/m². The meaning of the stiffness parameters E_{50}, E_{oed} and E_{ur} is illustrated in Figure 1.

Table 1. Parameters for the HS model.

Basic model		loose	dense Hostun sand
γ	[kN/m³]	15.0	17.0
φ'	[°]	34.0	42.0
ψ	[°]	0.0	16.0
c'	[kN/m²]	0.0	0.0
E_{50}^{ref}	[MN/m²]	12.0	30.0
E_{oed}^{ref}	[MN/m²]	16.0	30.0
m	[-]	0.75	0.55
E_{ur}^{ref}	[MN/m²]	60.0	90.0
ν_{ur}	[-]	0.25	0.25
Parameters for small-strain stiffness			
E_0^{ref}	[MN/m²]	170.0	270.0
$\gamma_{0.7}$	[-]	0.0002	0.0002

Table 2. Parameters for the hypoplastic model.

Basic model		Hostun sand
h_s	[MN/m³]	3800.0
φ_c	[°]	32.0
e_{c0}	[-]	0.91
e_{d0}	[-]	0.61
e_{i0}	[-]	1.09
n	[-]	0.29
α	[-]	0.134
β	[-]	1.35
Parameters for small-strain stiffness		
R	[-]	0.00006
m_R	[-]	5.0
m_T	[-]	2.0
β_r	[-]	0.5
χ	[-]	2.0

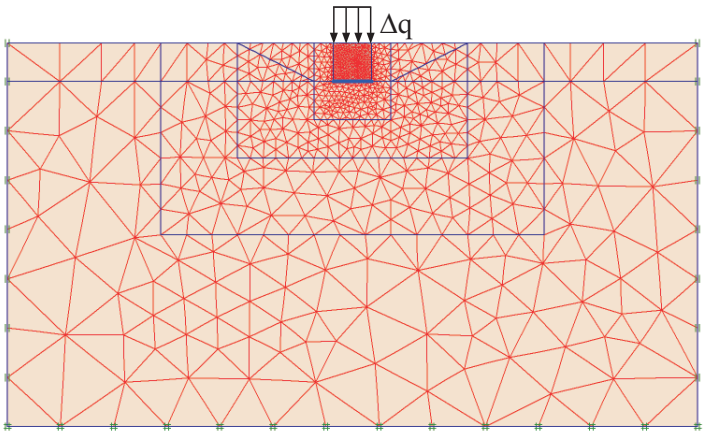

Figure 2. FE mesh of the strip footing.

4 LIMIT DEPTH

Classical settlement analyses need a limit depth in order not to overestimate the settlements. According to Tomlinson (1995) and the German code of practice DIN 4019 (1979) the limit depth is the depth where the additional stress due to the footing is twenty per cent of the initial effective vertical pressure.

Numerical calculations have been carried out for a one meter wide strip footing and for a circular footing with a diameter of one meter. Both are embedded one meter in dense Hostun sand (Fig. 2). To investigate the influence of the high stiffnesses at very small strains we will consider data for a footing pressure of 150 for the strip footing and 400 kN/m² for the circular footing in more detail.

Figures 3 and 4 show the vertical displacement over depth as resulting from the HS model, the HS-small model and the hypoplastic model. For the strip footing, it is observed that the influence of small-strain stiffness is considerable. The HS-model would seem to be out as it does not incorporate a small-strain stiffness. It can be seen that below a certain depth the vertical displacements tend to be negligibly small when small-strain stiffness is accounted for. One can observe that this depth is in good agreement with the limit depth in classical settlement analysis. Regarding the circular footing (Fig. 4) it can be seen that small-strain stiffness is not that important, since the HS and the HS-small model give nearly the same results.

Hence, the idea of a limit depth is well explained on the basis of small-strain stiffness, as also argued by Hintner et al. (2006). Another advantage of small-strain stiffness models is that numerical results depend no longer on the mesh size being special for plane strain problems. For numerical settlement analyses that do not consider the effect of small-strain stiffness, it is recommended to use a limit depth. And this limit depth can be taken according classical settlement analysis, e.g. according to the 20% rule.

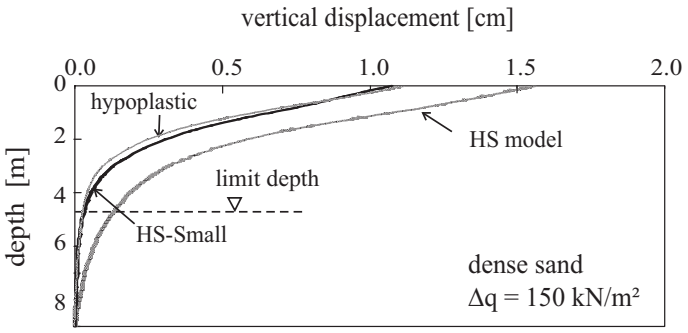

Figure 3. Vertical displacement over depth for strip footing.

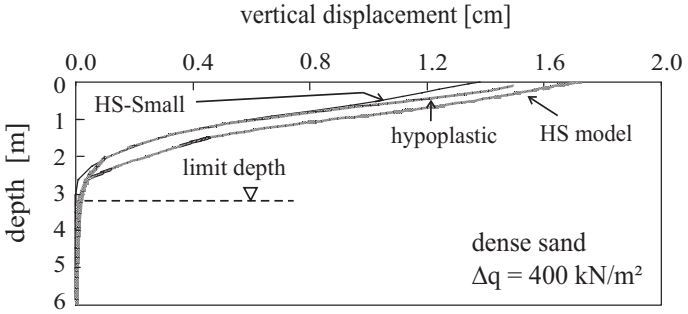

Figure 4. Vertical displacement over depth for circular footing.

5 BEARING CAPACITY OF INCLINED LOADS

5.1 *Analytical methods*

For a strip footing the well-known bearing capacity equation for inclined loading reads:

$$q_f = c' \cdot N_c \cdot i_c + q_0 \cdot N_q \cdot i_q + \gamma \cdot b \cdot N_b \cdot i_\gamma \qquad (1)$$

where N_c, N_q and N_b are friction dependent bearing capacity factors, c' is the effective cohesion, q_0 is the overburden pressure at foundation level and γ is the density of the soil below foundation level. In literature one often finds a different notation with $N_b = ½ N_\gamma$.

The bearing capacity equation is well-established, but varying expressions can be found for the inclination factors i_c, i_q and i_γ. Moreover, N_b or N_γ factors are computed in a different way depending on the country considered. Within this study the bearing capacity according the German standard DIN 4017 (2001) is used for the comparison to numerical calculations. Note that this code of practice is based on Meyerhof (1962) for the N_b factors.

5.2 *Numerical simulations for inclined loading*

The numerical calculations for the one meter wide strip footing were performed with a plane-strain mesh (Fig. 5) The ground is represented by 6-noded triangular elements. The boundary conditions of the finite element mesh are as follows: The ground surface is free to displace, the side surfaces have roller

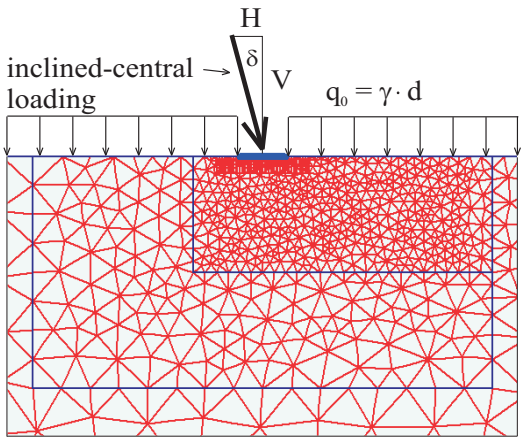

Figure 5. FE mesh of the strip footing with inclined loads.

boundaries and the base is fixed. The embedment of one meter is simulated with the overburden pressure q_0. Note that also the analytical approaches neglect the soil strength of the overburden. The footing itself behaves rigid. Between soil and foundation interface elements are us ed with contact friction equal to soil friction. The load has a constant inclination angle δ with respect to the vertical axis.

Numerical analysis of bearing capacity require soil models that should accurately simulate the soil strength. Since the Mohr-Coulomb model and the HS-small model are based on the same failure criterion the calculations have been carried out with the simple Mohr-Coulomb model and the hypoplastic model.

5.3 *Failure envelope for inclined loads*

Figures 6 and 7 show the envelopes of ultimate loads for the strip footing carried out with the Mohr-Coulomb model, the hypoplastic model and the analytical method according the German code of practice for loose as well as dense Hostun sand. It is observed that the Mohr-Coulomb and the analytical method give more or less the same envelope, but Mohr-Coulomb model is slightly more conservative. The hypoplastic model gives significantly higher ultimate loads; in the range of 20% for the dense sand and around 30% for the loose sand.

The difference between the two models results from the different failure surface since the hypoplastic model is based on Matsuoka & Nakai criterion (von Wolffersdorff 1996). Only under triaxial conditions both the Mohr-Coulomb and the Matsuoka & Nakai failure criterion give the same friction angle. For any other conditions the Mohr-Coulomb failure criterion yields to lower strength. Figures 6 and 7 show also that the shapes of the failure envelope for both the numerical and analytical methods are similar. These figures show the normalised ultimate loads, where V_0 is the bearing capacity for the vertical loading.

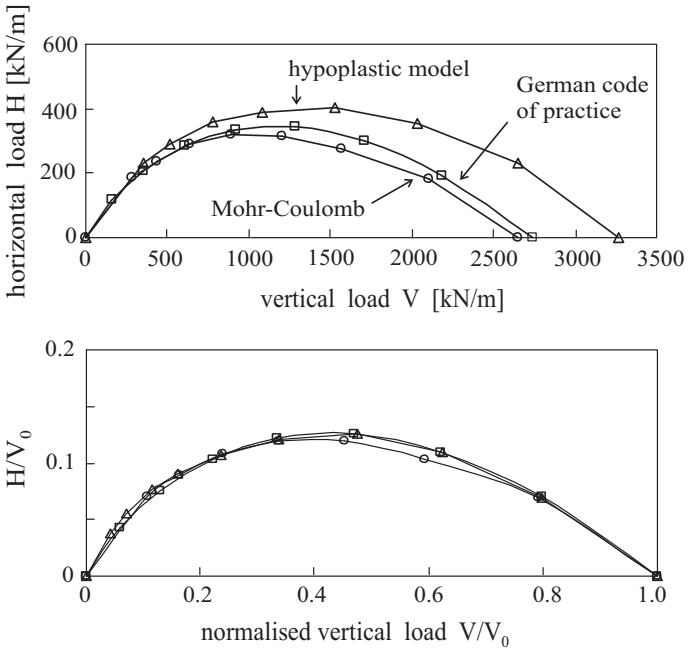

Figure 6. Failure envelope for the strip footing on dense sand.

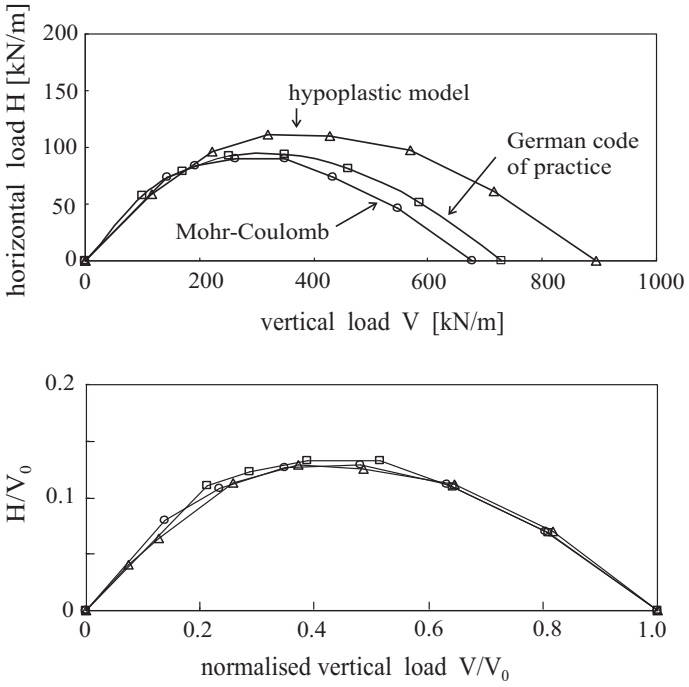

Figure 7. Failure envelope for the strip footing on loose sand.

6 DISPLACEMENT BEHAVIOUR OF A STRIP FOOTING ON SAND

Numerical calculations have also been performed to investigate the displacement of the strip footing for different loading paths. Figure 8 shows the displacement trajectories for two completely different paths of loading, namely for an inclined loading (I-C) and for horizontal loading (V-H). The loading paths have been chosen such there is the same load inclination at failure. At failure an inclination angle of $\delta = 20°$ is achieved.

As one can see in Figure 8, the vertical displacement is nearly the same, whereas the horizontal displacements differ by a factor of approximately 2. The difference is not a surprise. During I-C loading horizontal displacement occurs from beginning of loading. For V-H loading the soil has an increased stiffness after vertical loading and therefore the horizontal displacement is much lower than in the I-C case.

From Figure 8 it can be observed that the displacement increments at failure have the same direction. Hence, the displacement increments at failure are load path independent. The directon of the displacement increments are plotted in Figure 9. One can observe a non-associated flow rule for the displacement increments at failure. The angle between the normal line and the increments can be expressed with $\varphi' - \psi$. For the loose sand with dilatancy angle $\psi = 0$ one gets the friction angle φ'.

The angle $\varphi' - \psi$ is also found between the strain increment and the normal line in the direct shear test of a dense sand (Fig. 10).

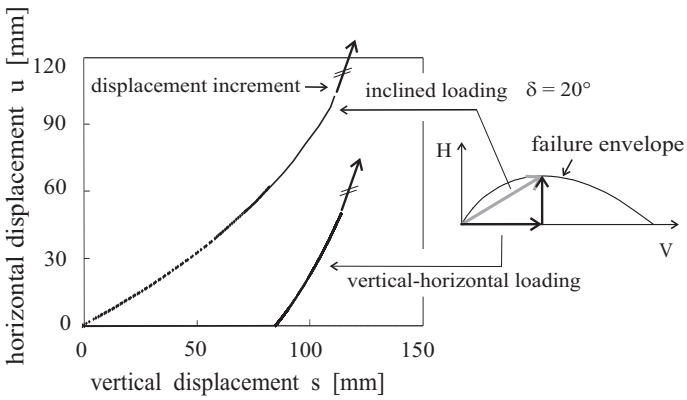

Figure 8. Displacement trajectories for 2 different load paths.

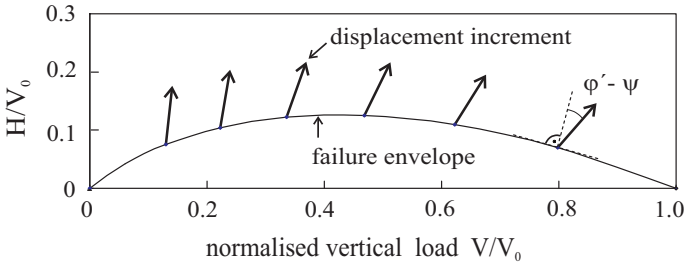

Figure 9. Displacement increments at failure (dense sand).

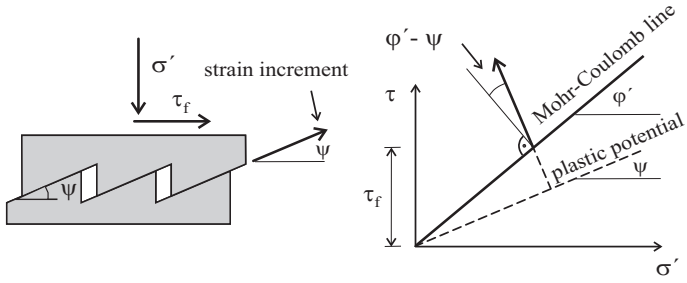

Figure 10. Analogy to plasticity theory.

7 ELASTIC SOLUTION FOR HORIZONTAL DISPLACEMENT PREDICTION

7.1 *Elastic solution for horizontal displacement*

According to Eurocode 7 (e.g Orr & Farrell 1999) the elasticity based settlement analysis is still state of the art in geotechnical engineering. One method is the adjusted elasticity method (Tomlinson 1995) that is based on the following equation:

$$s = \frac{1-\nu^2}{E} \cdot \Delta q \cdot b \cdot f \qquad (2)$$

where E is the Young´s Modulus, ν is the Poisson´s ratio, Δq is the net foundation pressure, b is the width of foundation, and f is the influence factor. The Young´s modulus of the soil may be estimated from the results of back-analyses, or from laboratory or in situ tests.

In this study we consider such a formula also for the horizontal displacement due to horizontal loads. Giroud (1969) gives an expression for the horizontal displacement due to uniform horizontal loading on an infinite elastic layer. This equation may be extended to finite elastic layers:

$$u = \frac{1}{2G} \cdot \tau \cdot b \cdot f_h \qquad with \qquad G = \frac{E}{2(1+\nu)} \qquad (3)$$

where u is the horizontal displacement, τ is the average applied shear stress and f_h is the influence factor. This factor depends on the b/h ratio, where b is the width of the foundation and h is the height of the compressible layer as indicated in Figure 11. In practice the depth h is either a physical layer thickness or the limit depth as described before. The influence factor f_h has been obtained from FE-computations for rigid footings on an elastic subsoil and results are shown in Table 3.

The shear modulus G in equation 3 may be computed from the constrained modulus E_{oed} (also denoted as M) via the Poisson ratio $\nu = 0.3$. Within this study E_{oed} is the tangent oedometer modulus due to the vertical stress at the end of vertical loading in a representative point under the footing. This vertical stress consists of the initial effective vertical pressure and the additional stresses due to loading. The additional stresses can be obtained on the basis of tables or graphs according Steinbrenner (1934).

The representative point is located the width b below the footing as suggested by the authors. One can see that this fitting is satisfactorily regarding Figure 12 that shows E_{oed} over depth for the vertical load V = 117 kN/m.

7.2 *Numerical calculations*

The numerical calculations have been carried out with the HS-small model and the hypoplastic model, both models extended by high stiffnesses at very small strains. The FE simulation is according the FE calculations for determining the bearing capacity as described before. First the vertical load is applied and then horizontal loading up to failure begins keeping the vertical load constant. No eccentricity is considered.

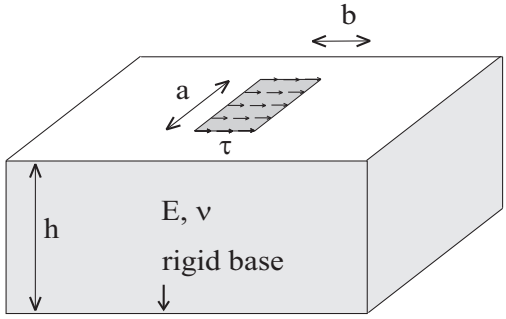

Figure 11. Elastic solution for horizontal displacement.

Table 3. Influence factors f_h for rigid footings and $\nu = 0.3$.

rigid	a/b = 1	a/b = 2	a/b = 3	a/b = 5	a/b = ∞
h/b = 0.5	0.62	0.67	0.67	0.67	0.67
h/b = 1.0	0.77	0.90	0.94	0.96	0.95
h/b = 1.5	0.83	1.01	1.08	1.12	1.13
h/b = 2.0	0.86	1.07	1.16	1.23	1.25
h/b = 3.0	0.89	1.13	1.25	1.36	1.43
h/b = 5.0	0.92	1.18	1.32	1.47	1.66

Figures 13 and 14 show the load-displacement curves obtained by the numerical analyses and by the elastic solution for different vertical loads for dense as well as loose sand. For the loose sand there is a good agreement between the two different models. For the dense sand however, the hypoplastic model behaves slightly softer than the HS model. Of course they behave different close to failure as already observed for the bearing capacity problem.

The load-displacement curve for the elastic solution is linear since the E-modulus obtained from vertical stresses in the soil remains constant during horizontal loading. Furthermore the elastic solution appears to be a good method for predicting horizontal displacements under horizontal working loads.

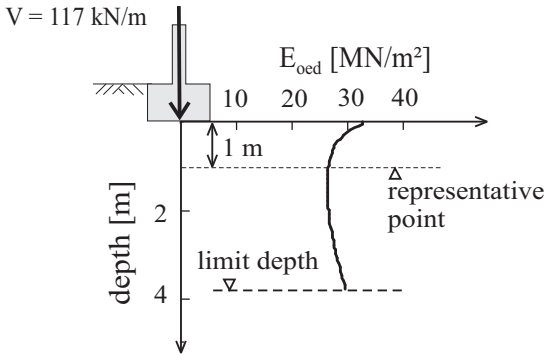

Figure 12. Representative point and E_{oed}.over depth.

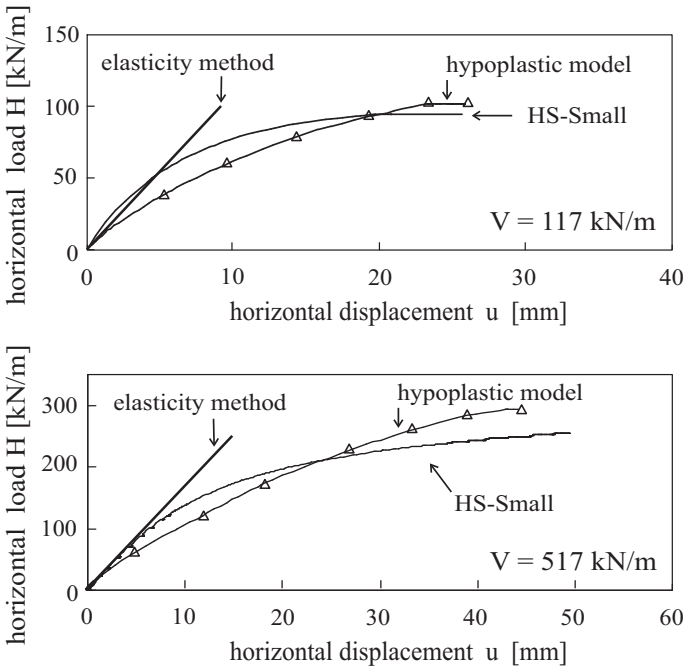

Figure 13. Horizontal load-displacement (dense sand).

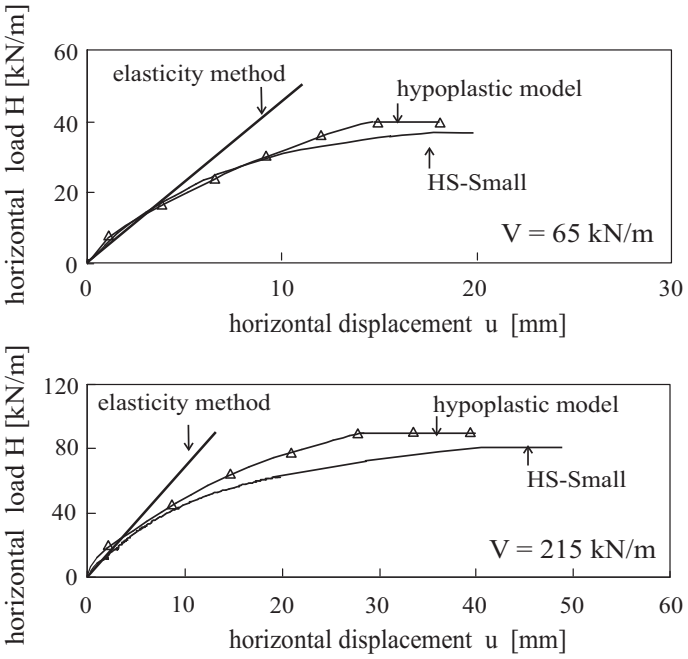

Figure 14. Horizontal load-displacement (loose sand).

8 CONCLUSIONS

This study comprehends the comparison of two completely different soil models namely the elast-plastic HS-small model and an hypoplastic model. Both are extended to include the effects of small-strain stiffness. At failure they differ as they are based on different failure criterions. But for working load level they give fairly similar results as already presented by Hintner et al. (2006) for vertical loading.

For the bearing capacity problem the paper shows good agreement between conventional geotechnical design and numerical results as based on a Mohr-Coulomb failure criterion. The hypoplastic model based on Matsuoka & Nakai criterion gives higher ultimate loads for the strip footing problem. But this is in accordance to Wroth (1984) who proposed for relating plane strain results the linear relationsship $8\varphi'_{ps} \approx 9\varphi'_{tc}$ where φ'_{ps} is the plane strain friction angle and φ'_{tc} is the triaxial compression friction angle.

Within this study an equation derived from elasticity theory to predict horizontal displacement is presented and it seems that this method would be useful in geotechnical engineering practice for easy loading conditions.

ACKNOWLEGDEMENT

The authors are indebted to Dr Thomas Benz for developing the HS-small model.

REFERENCES

Benz, T. 2006. Small-Strain Stiffness of Soils and its Numerical Consequences, *Ph.D. Thesis*. Mitteilung des Instituts für Geotechnik der Universität. Heft 56

DIN 4017, 2001. Soil - Calculation of design bearing capacity of soil beneath shallow foundations. Berlin: Beuth Verlag

DIN 4019, Part 1 1979. Subsoil; analysis of settlements for vertical and centric loading. Berlin: Beuth Verlag

Giroud, J.P. 1969. Déplacement horizontal d'une droite particulière de la surface d'un massif élastique semi-infini lineairement chargé. *C.R. Acad.Sc. Paris,* t.268, Série A: 252-255

Hintner, J. Vermeer, P.A. Baun, C. 2006. Advanced FE versus classical settlement analyses,. In H.F. Schweiger (ed), *proc. Num. Methods in Geotechn. Eng., Graz, 6-9 September 2006:* 539-546. Rotterdam Balkema

Kolymbas, D. 1991. An outline of hypoplasticity. *Archive Applied Mechanics* 61: 143-151

Meyerhof, G.G. 1962. Neue Forschungen über die Tragfähigkeit von Flachgründungen und Plattengründungen. Mitteilungen aus dem Institut für Verkehrswasserbau, Grundbau und Bodenmechanik der TH Aachen, Heft 25

Niemunis, A. Herle, I. 1997. Hypoplastic model for cohesionless soils with elastic strain range, *Mechanics of Cohesive Frictional Materials*,Vol. 2: 279-299

Orr, T.L.L., Farrell E.R. 1999. Geotechnical Design to Eurocode 7. London: Springer-Verlag

Schanz T. 1998. Zur Modellierung des mechanischen Verhaltnes von Reibungsmaterialien. *Habilitation.* Mitteilung des Instituts für Geotechnik der Universität, Heft 45

Steinbrenner, W. 1934. Tafeln zur Setzungsberechnung. *Straße* 1: 121-124

Tomlinson, M.J. 1995. Foundation Design and Construction Sixth Edition. Longman

Vermeer P.A. 1978. A double hardening model for sand. *Geotéchnique* 28: 413-433

Von Wolffersdorff, P.-A. 1996. A hypoplastic constitutive relation for granular materials with a predefined limit state surface. *Mech. of Cohes. Frict. Mater.*, Vol. 1: 251-271

Wroth, C.P. 1984. The interpretation of in situ soil tests. *Geotéchnique* 34 (4): 449-489